Journal of Molecular Catalysis A: Chemical 350 (2011) 91–96

Contents lists available at SciVerse ScienceDirect

Journal of Molecular Catalysis A: Chemical

journal homepage: www.elsevier.com/locate/molcata

Enhanced electrocatalytic activity of a new carbon nanocomposite electrode based on organic–inorganic hybrid nanostructures

Afsaneh Safavi[a,b,*], Elaheh Farjami[a,b]

[a] Department of Chemistry, College of Sciences, Shiraz University, Shiraz 71454, Iran
[b] Nanotechnology Research Institute, Shiraz University, Shiraz, Iran

ARTICLE INFO

Article history:
Received 17 April 2011
Received in revised form
14 September 2011
Accepted 17 September 2011
Available online 23 September 2011

Keywords:
Organic–inorganic hybrid nanocomposite electrode
Electrocatalytic activity
Oxygen reduction reaction
Hydrogen evolution
Hydrazine oxidation

ABSTRACT

Organic–inorganic hybrid nanostructures are successfully synthesized by incorporating 3,3′,5,5′-tetramethylbenzidine (TMB) and palladium chloride ($PdCl_2$) at room temperature. The general morphology of the product was characterized by transmission electron microscopy (TEM) which displayed Pd distributed in the TMB matrix. A novel nanocomposite electrode was constructed by incorporation of the as-prepared product into carbon ionic liquid electrode (CILE). After reduction of Pd(II) to Pd(0) during a negative reduction pulse; the electrocatalytic properties of the composite electrode were investigated towards oxygen reduction, hydrogen evolution and hydrazine oxidation all of which revealed strong electrocatalytic activities at room temperature.

1. Introduction

Palladium nanostructures have received significant interest in the recent years [1–3] due to their superior catalytic performance towards various chemical and electrochemical reactions such as catalysis [4,5], hydrogen storage [6,7], and sensors [8,9].

While platinum is the most extensively used noble metal for catalysis at different areas, its high price is a major restriction factor on its utility as an electrocatalyst. Much effort has been devoted to minimize the Pt loading and to achieve optimum performance [10]. Therefore, Pd-based catalysts might be a promising substitute for Pt because of lower costs and more abundance in nature which could be used without compromising on catalytic activity.

The size and shape of the nanostructures strongly affect their catalytic and electrocatalytic performance [11,12]. Thus, it is important to prepare Pd nanostructures on a suitable matrix to exploit the high surface-area-to-volume ratio and enhanced catalytic activity.

Most of the methods for the preparation of Pd nanostructures are either solution based or coated on suitable substrates [13–15]. Carbon-based supports are generally used for dispersing the nanoparticles and to achieve very high catalytic activity [16]. Moreover, conducting polymers can be extensively used due to their lower ohmic drop across the electrode. Also, their easy functionalization with biomolecules make them as an effective substitute for carbon-based supports and applicable as sensors [16,17].

On the other hand, one-dimensional (1D) organic–inorganic hybrid nanomaterials based on the combination of organic and inorganic species exhibit the advantages over organic (such as light weight, flexibility and good moldability) and inorganic (such as high strength, heat stability and chemical resistance) materials [18,19]. Hybrid materials range from simple mixtures of bulk materials to combine properties of inorganic and organic components down to the mixture of materials on the nanometer scale or even at molecular/ionic levels [20]. These, in fact represent one of the most promising classes of materials which have potential applications in chemical or biochemical sensors, catalysis, and nanodevices [21–23].

Variety of methods are developed to fabricate the organic–inorganic hybrid 1D nanostructures, such as electrospinning, template-directed growth, and sol–gel. These are usually complicated processes with limited practical applications [24–26]. Recently, a facile and efficient method based on a wet-chemical route [27] has been developed for the synthesis of organic–inorganic hybrid 1D nanostructures.

3,3′,5,5′-tetramethylbenzidine (TMB) with much less hazards than benzidine has an excellent coordination ability with

* Corresponding author. Tel.: +98 711 6137351; fax: +98 711 2286008.
E-mail address: safavi@chem.susc.ac.ir (A. Safavi).

1381-1169/$ – see front matter © 2011 Elsevier B.V. All rights reserved.
doi:10.1016/j.molcata.2011.09.012

transition metal ions [28]. Doping of TMB through the reaction between TMB and these ions could be used as an attractive route to fabricate inorganic–organic hybrid nanomaterials.

Incorporation of TMB and H_2PtCl_6 at room temperature has been recently reported to produce an organic–inorganic hybrid nanofiber by a wet-chemical route which displays a strong fluorescence emission at room temperature that may be promising for applications in the fabrication of photoelectric materials [27]. Moreover, bimetallic Au-Pt nanoparticles/organic nanofibers with a three-dimensional (3D) structure has been developed in which the bimetallic Au-Pt nanoparticles are homogenously distributed in the matrix of interlaced organic nanofibers used for the electrochemical assay of Hg(II) [29].

Recently, we proposed carbon ionic liquid electrode (CILE) as a high performance electrode [30–32]. We also introduced a simple method for fabrication of arrays of palladium nanoparticles on this electrode and demonstrated its electrocatalytic behaviour towards oxygen reduction, hydrogen peroxide and hydrazine oxidation [33,34]. In these studies, palladium nanoparticles have been deposited on the CILE surface by electrodeposition method. However, the general drawback with electrodeposited nanostructures is their relatively low stability, especially when they are used in hydrodynamic methods where detachment of nanoparticles is most probable.

To the best of our knowledge there has been no report on the reaction of palladium ions with TMB as an organic matrix. Therefore, in this paper we describe a wet-chemical synthesis of organic–inorganic hybrid nanomaterial by incorporating TMB with $PdCl_2$ followed by mixing a known amount of the obtained product with ionic liquid and graphite in order to prepare a nanocomposite electrode based on organic–inorganic hybrid nanostructures. Here, Pd(II) ions in TMB-based organic network were reduced to metallic Pd during a sufficiently negative reduction pulse before each experiment. Furthermore, we investigated the excellent electrocatalytic activity of the resulting nanocomposite electrode for hydrogen evolution, oxygen reduction and hydrazine oxidation.

2. Experimental

2.1. Materials

All chemicals used were of analytical grade or of the highest purity available. 1-iodooctane, pyridine, absolute ethanol, TMB, hydrazine hydrochloride, palladium(II) chloride were obtained from Merck and used as received. Sulfuric acid (98%, AR) was obtained from Aldrich.

Ammonium hexafluorophosphate, and graphite powder (mesh size <100 μm) were supplied by Fluka. All other chemicals were analytical grade from Merck. Distilled deionized water was used to prepare all solutions.

The ionic liquid, octylpyridinium iodide was synthesized as described elsewhere [35]. Octylpyridinum hexafluorophosphate ($OPy^+PF_6^-$) was obtained by anion exchange of octylpyridinium iodide with ammonium hexafluorophosphate.

2.2. Apparatus

Voltammetric measurements were performed using an Autolab electrochemical system (Eco-Chemie, Utrecht, The Netherlands) equipped with Autolab type II and GPES software (Eco-Chemie). The electrochemical cell was assembled with a conventional three-electrode system: an Ag/AgCl/KCl (3M) reference electrode (Metrohm) and a platinum disk as a counter electrode. Different working electrodes used in this study were a CILE and Pd(II)-TMB/CILE nanocomposite electrode (1.8-mm diameter). The cell was a one-compartment cell with an internal volume of 10 mL. All experiments were typically conducted at room temperature.

A model CM10 transmission electron microscope (TEM, Philips) was used to characterize the product. X-ray diffraction (XRD) measurements were performed on a Thermoelectron instrument (VG multilab 2000).

2.3. Synthesis of Pd-TMB nanostructures

According to a synthesis method for Pt-TMB nanostructure reported previously [27]; in a typical experiment 1.25 mL of 4 mM $PdCl_2$ aqueous solution was added into 2 mL of 2.5 mM ethanolic TMB solution at room temperature. Several minutes later, the formation of a large amount of yellow–orange precipitate was observed with the naked eye. The precipitate was collected by centrifugation, washed several times with water and then dried at 50 °C.

2.4. Electrode preparation

Carbon ionic liquid electrode (CILE), 1.8 mm diameter, was prepared using graphite powder and $OPy^+PF_6^-$ with a ratio of 50/50 (w/w) as described previously [30].

The nanocomposite electrode was prepared by hand-mixing of weighed amounts of graphite powder, ionic liquid and the as-prepared Pd-TMB powder (50:45:5 wt%). A portion of the resulting paste was packed firmly into the cavity (1.8 mm i.d.) of a Teflon holder. The electric contact was obtained by smoothing the electrode onto a smooth paper.

Doped Pd(II) ions were reduced to Pd(0) during a negative reduction pulse; thus leading to a metallic Pd-TMB inorganic–organic hybrid nanocomposite.

3. Results and discussion

3.1. Characterization

It has been reported that TMB serves as an electron donor [27]. A color change occurred rather rapidly when $PdCl_2$ aqueous solution was added into ethanolic TMB solution. Similar to Pt [27,29], the general process for the formation of the organic–inorganic hybrid might involves the redox reaction between TMB and Pd(II) ions through partial oxidation of TMB and the simultaneous partial reduction (not all) of the metal ions to Pd(0) which can coordinate by nitrogen ligands of TMB [36,37].

The representative TEM image of the as-synthesized Pd/TMB based inorganic–ogranic hybrid nanocomposite is shown in Fig. 1, which exhibits the spherical shape of palladium distributed separately in TMB network matrix, each having a diameter of approximately 8 nm. X-ray diffraction (XRD) was used for investigation of the structure of the product (Fig. 2). XRD pattern shows the two broad peaks (Fig. 2a) observed at 2θ angles of 30° and 40° which can be ascribed to the formation of amorphous organic–inorganic hybrid structure. Although TEM image shows the spherical palladium particles, but the loading density of palladium particles in TMB network matrix in not sufficient to produce a significant peak corresponding to palladium particles in XRD (Fig. 2). Therefore, XRD pattern of the product mainly shows the formation of amorphous organic–inorganic hybrid structure.

Fig. 3 shows cyclic voltammograms of the prepared Pd-TMB/CILE in buffer (PBS pH 7.0). As it is seen only traces of Pd(0) is formed in the as-prepared Pd-TMB/CILE nanocomposite electrode (Fig. 3, curve b). However, after application of a reduction pulse at −0.80 V for 3 min, a significant amount of Pd(0) was formed on the electrode surface and therefore, the cyclic voltammogram related

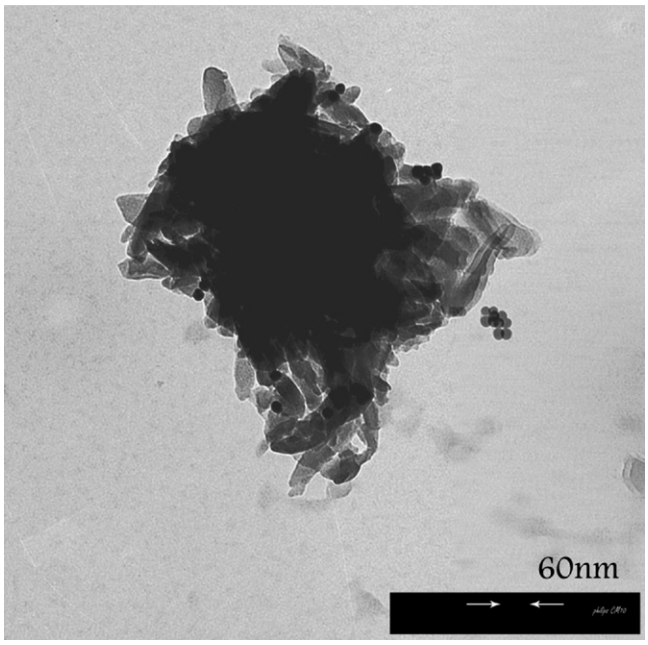

Fig. 1. TEM image of the as-prepared Pd/TMB organic–inorganic hybrid nanostructure.

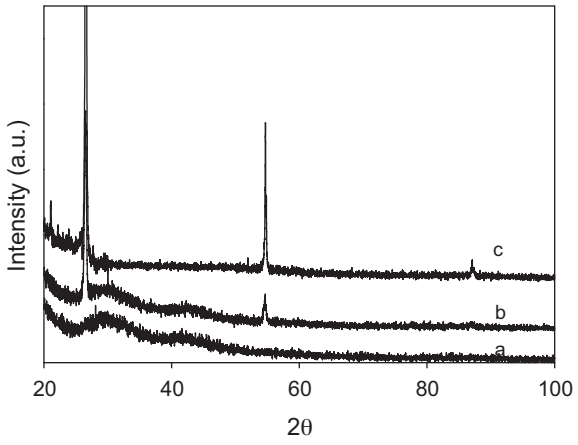

Fig. 2. XRD pattern of (a) the product Pd-TMB, (b) Pd-TMB/CILE, and (c) CILE.

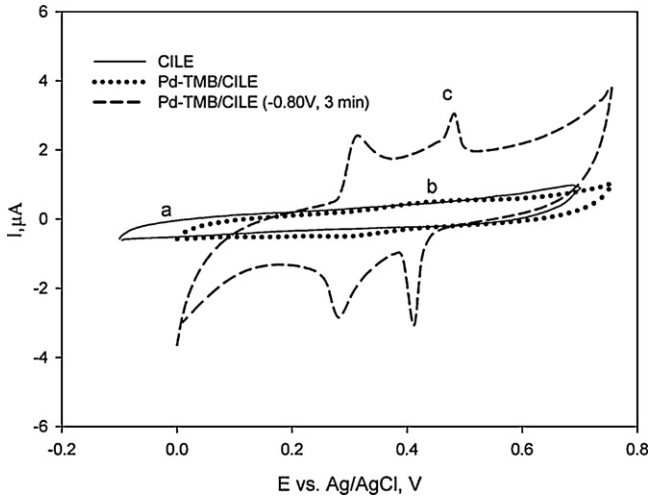

Fig. 3. Cyclic voltammograms recorded at (a) CILE, (b) Pd-TMB/CILE, and (c) Pd-TMB/CILE after applying a potential of −0.80 V for 3 min (Conditions: phosphate buffer (pH 7.0), scan rate of 100 mV s^{-1}).

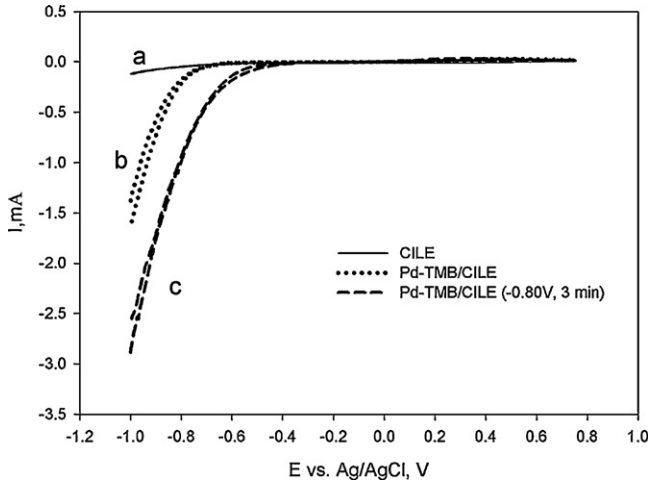

Fig. 4. Cyclic voltammograms recorded at (a) CILE, (b) Pd-TMB/CILE, and (c) Pd TMB/CILE after applying a potential of −0.8 V for 3 min (Conditions: 0.5 M H_2SO_4, scan rate of 100 mV s^{-1}).

to Pd(0) shows a pair of two significant peaks due to the oxidation and reduction of Pd(0) formed during a reduction pulse (curve c).

The existence of the Pd is also confirmed by two cathodic current peaks located between 0.60 and 0.20 V during the negative scan, which are probably attributed to the reduction of palladium oxides formed [38] at higher potentials during the positive scan (Fig. 3, curve c).

In order to clarify the presence of Pd nanoparticles, the catalytic activity of the as-prepared Pd-TMB/CILE nanocomposite was studied towards hydrogen evolution, oxygen reduction and hydrazine oxidation as test reactions.

3.2. Catalytic activity towards hydrogen evolution reaction

Palladium has a high potential to adsorb large quantities of hydrogen in bulk to form hydrides and therefore is well known as a hydrogen storage material [39].

Voltammograms (a–c) of Fig. 4 show respectively the voltammetric behaviour of the CILE, Pd-TMB/CILE and Pd-TMB/CILE (after treatment at −0.80 V for 3 min) in 0.5 M H_2SO_4 at a scan rate of 100 mV s^{-1}. Although, there is only traces of Pd(0) which is formed in the as-prepared Pd-TMB/CILE nanocomposite electrode; but a clear hydrogen evolution current was observed for Pd-TMB/CILE

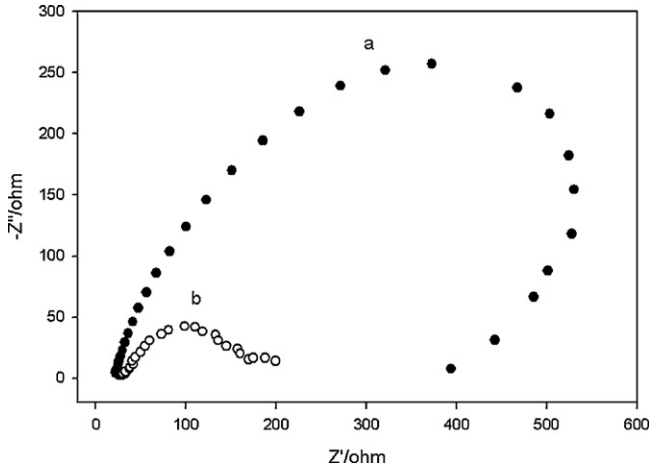

Fig. 5. The Nyquist plots for Pd-TMB/CILE in 0.5 M H_2SO_4 at −0.55 V (a) before and (b) after applying a reduction pulse (−0.80 V, 3 min).

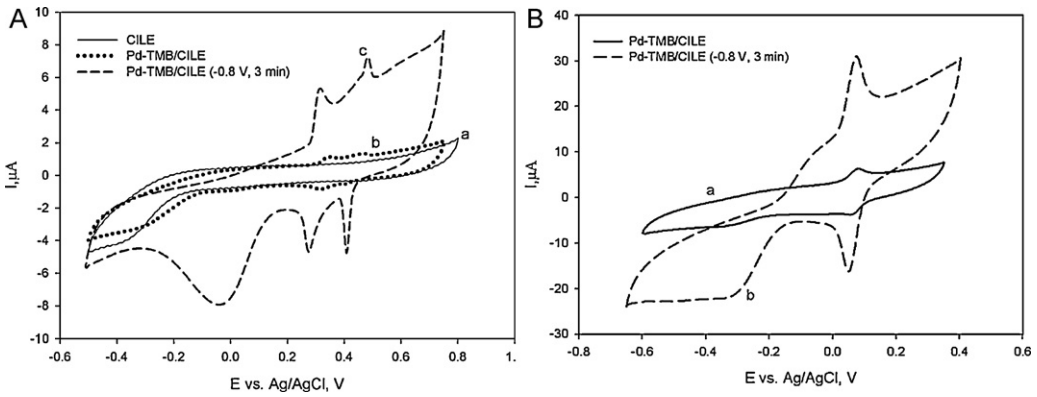

Fig. 6. Cyclic voltammograms for oxygen reduction reaction (A) in O_2-saturated phosphate buffer (pH 7.0) recorded at (a) CILE, (b) Pd(II)-TMB/CILE, (c) Pd-TMB/CILE after applying a reduction pulse (−0.80 V, 3 min) and (B) in 0.1 M NaOH at (a) Pd(II)-TMB/CILE, (b) Pd-TMB/CILE after applying a reduction pulse (−0.80 V, 3 min).

nanocomposite compared to CILE without any modification (Fig. 4). Although, more pronounced signal for hydrogen evolution was observed after reduction treatment of Pd-TMB/CILE at −0.80 V for 3 min. The measured onset potential (−0.40 V) is also significantly lower than −0.70 V observed for Pd-TMB/CILE before reduction at −0.80 V which indicates that Pd(II) in the TMB network matrix is reduced to Pd(0) during a reduction treatment.

In order to investigate the effect of reduction treatment, we carried out electrochemical impedance spectroscopy (EIS) in 0.5 M H_2SO_4 for the Pd-TMB/CILE nanocomposite. Fig. 5 shows the Nyquist plot of the nanocomposite electrode before and after electrochemical reduction treatment. The corresponding values of Nyquist plot measured at the lowest frequency show (semicircle diameter) that the impedance decreases dramatically after reduction step, thereby confirming the facile nature of the electron-transfer process.

3.3. Catalytic activity towards oxygen reduction reaction

According to the previous studies, Pd presents a high activity towards oxygen reduction reaction (ORR) [40,41]. Therefore, the ORR tests were conducted in O_2-saturated aqueous solutions (PBS, pH 7.0) on CILE, Pd(II)-TMB/CILE and Pd(0)-TMB/CILE. These results exhibit a well positive shift and high eletrocatalytic effect for ORR on the surface of Pd(0)-TMB/CILE nanocomposite. Moreover, a dramatic increase in the peak current (Fig. 6), along with a great improvement in the peak shape after reduction of Pd(II) to Pd(0) is observed which shows improved electrocatalytic properties.

Catalytic response for oxygen reduction reaction was also observed in alkaline solution (Fig. 6B). However, in acidic solution catalytic signal was overlapped with two cathodic peaks corresponding to palladium which is present as a catalyst in the electrode.

3.4. Catalytic activity towards hydrazine oxidation

Hydrazine and its derivatives have been recognized as environmental pollutants by Environmental Protection Agency (EPA) [42] and also as a neurotoxin and human carcinogen compound that can be absorbed through skin which could affect the liver, kidney and the brain [43]. Although electrocatalytic oxidation of hydrazine has been studied on different electrodes modified using catalysts such as ZnO nanostructures [44,45], gold nanoparticles [46,47], nickel hexacyanoferrate [48] and silver nanoparticles [49]; palladium nanoparticles show higher electrocatalytic behaviour for electrooxidation of hydrazine. In most previous reports, palladium has been deposited on a variety of substrates [1,50], but the general drawback with electrodeposited nanostructures is their relatively low stability due to detachment of nanoparticles.

In this work, the electrocatalytic activity of Pd(0)-TMB/CILE nanocomposite towards oxidation of hydrazine has been evaluated as a model system.

Fig. 7A shows the cyclic voltammogram of hydrazine at the Pd-TMB/CILE in phosphate buffer solution (PBS, pH 7.0) compared to CILE without any modifications. The peak potential for the hydrazine electro-oxidation on Pd(0)-TMB/CILE was found to be around −0.05 V, which is more negative than the values reported in the literature for the hydrazine electro-oxidation in phosphate buffer medium [34,50–52]. From these observations, it is obvious that the huge enhancement in hydrazine oxidation current on

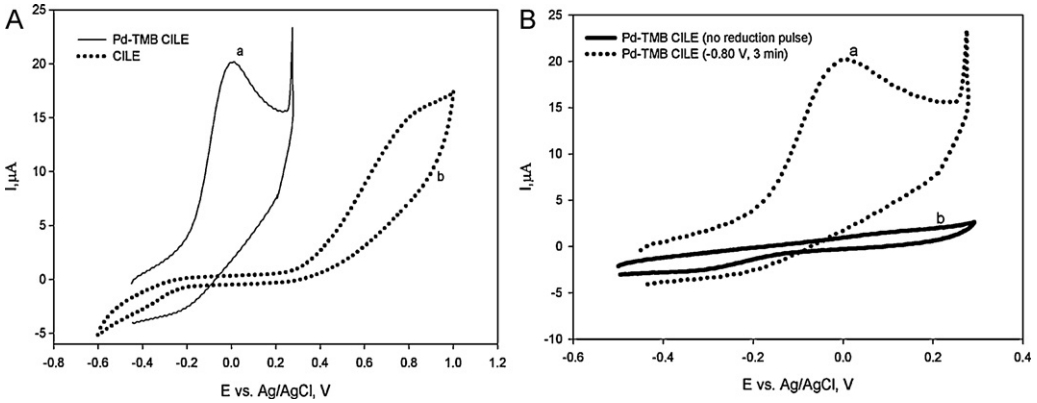

Fig. 7. Cyclic voltammograms of 1 mM hydrazine in phosphate buffer solution (pH 7.0) (A) at (a) Pd-TMB/CILE after applying a reduction pulse (−0.8 V, 3 min) and (b) CILE; (B) Comparison of responses of (a) Pd-TMB/CILE after applying a reduction pulse (−0.80 V, 3 min) and (b) the as-prepared Pd(II)-TMB/CILE.

Pd-TMB/CILE is due to the electrocatalytic effect of Pd nanoparticles. Such a voltammetric response was not observed at Pd(II)-TMB/CILE without any treatment (Fig. 7B), confirming the importance of the presence of Pd(0) in the composite during the reduction pulse.

Catalytic oxidation signal for hydrazine was also studied by changing pH values from 8.7 to 4. Although in more basic solutions the catalytic oxidation peak appeared at more negative potentials, but the catalytic oxidation current decreased at pH values above 7.5. By changing pH from 7 to more acidic values; the analytical signal corresponding to hydrazine oxidation appeared in the same region as stripping potential of palladium metal from the electrode surface; consequently the analytical signal for hydrazine oxidation decreased gradually.

A plot of electrocatalytic oxidation peak current versus square root of scan rate ($\upsilon^{1/2}$) yielded a straight line indicating a diffusion-controlled electron transfer mechanism for the hydrazine oxidation reaction at the Pd(0)-TMB/CILE.

In order to compare the prepared electrodes with bare CILE and to electrochemically characterize the real surface of the Pd(0)-TMB/CILE, 1mM hydrazine in phosphate buffer solution (pH 7.0) was used as the probe. From the cyclic voltammetric peak current and the diffusion coefficient of hydrazine reported in literature [47], the surface area of the electrode was calculated by using the following equation [53]:

$$i_{Pa} = (2.69 \times 10^5) n^{3/2} A D_0^{1/2} \nu_0^{1/2}$$

where n is the number of electrons transferred, i.e. 4 (assuming a 4 electrode transfer process mechanism of hydrazine oxidation on carbon electrodes [54]), A the geometric surface area of the electrode, D_0 the diffusion coefficient ($4.1 \times 10^{-5}\ cm^{-2}\ s^{-1}$) [47], υ the scan rate ($100\ mV\ s^{-1}$), and C_0^* the concentration of electroactive species (1 mM). The real surface area of Pd(0)-TMB/CILE electrode was found to be 0.21 cm^2, while that of the bare CILE was 0.06 cm^2. The surface area of Pd(0)-TMB/CILE was estimated to be about 3.5 times that of the bare CILE.

3.5. Stability of the electrocatalyst

As-synthesized Pd/TMB was kept in an airtight box. Also, the as-prepared Pd-TMB/CILE nanocomposite electrode was stored in air at ambient and its stability was checked every 10 days. The electrocatalytic responses of the proposed nanocomposite electrode (with 5% of electrocatalyst) towards hydrazine, oxygen reduction and hydrogen evolution were 90%, 82% and 86% of its initial values after 45 days, respectively. Along with good stability, the prepared nanocomposite electrode can be reused by simple polishing and not further treatment, even after 45 days.

4. Conclusion

Pd(II)-TMB organic–inorganic hybrid nanostructures have been successfully synthesized by incorporating TMB with $PdCl_2$ under ambient conditions.

We have constructed a new nanocomposite electrode by incorporating a small amount of the as-prepared hybrid nanostructures into the carbon ionic liquid electrode followed by the reduction of Pd(II) to Pd(0). Regardless of the low Pd loading in the nanocomposite electrode, the proposed nanocomposite electrode exhibits very good electrocatalytic activity and acts as an effective electrocatalyst for the hydrogen evolution, oxygen reduction reaction and hydrazine electro-oxidation.

Acknowledgements

The authors wish to express their gratitude to the Third World Academy of Sciences Iran Chapter (TWASIC) and Shiraz University Research Council for the support of this work.

References

[1] D.J. Guo, H.L. Li, Electrochem. Commun. 6 (2004) 999–1003.
[2] X.R. Ye, Y. Lin, C. Wang, M.H. Engelhard, Y. Wang, C.M. Wai, J. Mater. Chem. 14 (2004) 908–913.
[3] N. Tian, Z. Zhou, N. Yu, L. Wang, S. Sun, J. Am. Chem. Soc. 132 (2010) 7580–7581.
[4] B.J. Gallon, R.W. Kojima, R.B. Kaner, P.L. Diaconescu, Angew. Chem. Int. Ed. 46 (2007) 7251–7254.
[5] J. Hu, Y. Liu, Langmuir 21 (2005) 2121–2123.
[6] H.P. Liang, N.S. Lawrence, L.J. Wan, L. Jiang, W.G. Song, T.G.J. Jones, J. Phys. Chem. C 112 (2008) 338–344.
[7] H. Kobayashi, M. Yamauchi, H. Kitagawa, Y. Kubota, K. Kato, M. Takata, J. Am. Chem. Soc. 130 (2008) 1828–1829.
[8] F.J. Ibanez, F.P. Zamborini, J. Am. Chem. Soc. 130 (2008) 622–633.
[9] P. Zhou, Z. Dai, M. Fang, X. Huang, J. Bao, J. Gong, J. Phys. Chem. C 111 (2007) 12609–12616.
[10] R.K. Pandey, V. Lakshminarayanan, J. Phys. Chem. C 113 (2009) 21596–21603.
[11] R. Narayanan, M.A. El-Sayed, Nano Lett. 4 (2004) 1343–1348.
[12] C. Wang, H. Daimon, Y. Lee, J. Kim, S. Sun, J. Am. Chem. Soc. 129 (2007) 6974–6975.
[13] W. Pan, X. Zhang, H. Ma, Z. Zhang, J. Phys. Chem. C 112 (2008) 2456–2461.
[14] V. Mazumder, S. Sun, J. Am. Chem. Soc. 131 (2009) 4588–4589.
[15] L. Xiao, L. Zhuang, Y. Liu, J. Lu, H.D. Abruna, J. Am. Chem. Soc. 131 (2009) 602–608.
[16] R.K. Pandey, V. Lakshminarayanan, J. Phys. Chem. C 114 (2010) 8507–8514.
[17] H. Mao, X. Lu, X. Liu, J. Tang, C. Wang, W. Zhang, J. Phys. Chem. C 113 (2009) 9465–9472.
[18] C. Sanchez, B. Julian, P. Belleville, M. Popall, J. Mater. Chem. 15 (2005) 3559–3592.
[19] J.W. Kriesel, T.D. Tilley, Adv. Mater. 15 (2003) 1645–1648.
[20] T. Yoshida, J. Zhang, D. Komatsu, S. Sawatani, H. Minoura, T. Pauporté, D. Lincot, T. Oekermann, D. Schlettwein, H. Tada, D. Wöhrle, K. Funabiki, M. Matsui, H. Miura, H. Yanagi, Adv. Funct. Mater. 19 (2009) 17–43.
[21] A.L. Briseno, S.C.B. Mannsfeld, X. Liu, Y. Xiong, S.A. Jenekhe, Z. Bao, Y. Xia, Nano Lett. 7 (2007) 668–675.
[22] R.J. Tseng, J. Huang, J. Ouyang, R.B. Kaner, Y. Yang, Nano Lett. 5 (2005) 1077–1080.
[23] J. Polleux, A. Gurlo, N. Barsan, U. Weimar, M. Antonietti, M. Niederberger, Angew. Chem. Int. Ed. 45 (2006) 261–265.
[24] J. Huang, I. Ichinose, T. Kunitake, Angew. Chem. Int. Ed. 45 (2006) 2883–2886.
[25] D. Wang, Y.L. Chang, Z. Liu, H. Dai, J. Am. Chem. Soc. 127 (2005) 11871–11875.
[26] K.J.C. Bommel, A. Friggeri, S. Shinkai, Angew. Chem. Int. Ed. 42 (2003) 980–999.
[27] J. Yang, H. Wang, L. Lu, Y. Wang, W. Shi, H. Zhang, Synth. Met. 158 (2008) 572–576.
[28] V.R. Holland, B.C. Saunders, F.L. Rose, A.L. Walpole, Tetrahedron 30 (1974) 3299–3302.
[29] J. Gong, T. Zhou, D. Song, Li. Zhang, X. Hu, Anal. Chem. 82 (2010) 567–573.
[30] N. Maleki, A. Safavi, F. Tajabadi, Anal. Chem. 78 (2006) 3820–3826.
[31] A. Safavi, N. Maleki, F. Tajabadi, Analyst 132 (2007) 54–58.
[32] A. Safavi, N. Maleki, O. Moradlou, F. Tajabadi, Anal. Biochem. 359 (2006) 224–229.
[33] A. Safavi, N. Maleki, F. Tajabadi, E. Farjami, Electrochem. Commun. 9 (2007) 1963–1968.
[34] N. Maleki, A. Safavi, E. Farjami, F. Tajabadi, Anal. Chim. Acta 611 (2008) 151–155.
[35] E. Fisicaro, A. Ghizzo, E. Pelizzetti, G. Viscaradi, P.L. Quagliotto, J. Colloid Interface Sci. 182 (1996) 549–557.
[36] A. Mederos, S. Domĭnguez, R. Hernĭ andez-Molina, J. Sanchiz, F. Brito, Coord. Chem. Rev. 193 (1999) 857–911.
[37] X. Sun, S. Dong, E. Wang, J. Am. Chem. Soc. 127 (2005) 13102–13103.
[38] L. Jiang, A. Hsu, D. Chu, R. Chen, Electrochim. Acta 55 (2010) 4506–4511.
[39] Y. Gimeno, A.H. Creus, S. Gonzalas, R.C. Salvarezza, A. Arvia, J. Chem. Mater. 13 (2001) 1857–1864.
[40] L. Jiang, A. Hsu, D. Chu, R. Chen, J. Electrochem. Soc. 156 (2009) B370–B376.
[41] Y.F. Yang, Y.H. Zhou, C.S. Cha, Electrochim. Acta 40 (1995) 2579–2586.
[42] S. Amlathe, V.K. Gupta, Analyst 113 (1988) 1481–1483.
[43] S. Garrod, M.E. Bollard, A.W. Nicholls, S.C. Connor, J. Connelly, J.K. Nicholson, E. Holmes, Chem. Res. Toxicol. 18 (2005) 115–122.
[44] A. Umar, M.M. Rahman, S.H. Kim, Y.-B. Hahn, Chem. Commun. 2 (2008) 166–168.
[45] A. Umar, M.M. Rahman, Y.-B. Hahn, Talanta 77 (2009) 1376–1380.
[46] J. Li, X. Lin, Sens. Actuators B 126 (2007) 527–535.
[47] M. Hosseini, M.M. Momeni, M. Faraji, J. Mol. Catal. A: Chem. 335 (2011) 199–204.
[48] A. Salimi, K. Abdi, Talanta 63 (2004) 475–483.

[49] Q. Yi, L. Li, W. Yu, Z. Zhou, G. Xu, J. Mol. Catal. A: Chem. 295 (2008) 34–38.
[50] X.B. Ji, C.E. Banks, W. Xi, S.J. Wilkins, R.G. Compton, J. Phys. Chem. B 110 (2006) 22306–22309.
[51] C.C. Yang, A.S. Kumar, M.C. Kuo, S.H. Chien, J.M. Zen, Anal. Chim. Acta 554 (2005) 66–73.
[52] X. Dai, G.G. Wildgoose, R.G. Compton, Analyst 131 (2006) 1241–1247.
[53] A.J. Bard, L.R. Faulkner, Electrochemical Methods Fundamentals and Applications, 2nd ed., Wiley, New York, 2004.
[54] C.B. McAuley, C.E. Banks, A.O. Simm, T.G.J. Jones, R.G. Compton, Analyst 131 (2006) 106–110.